

Investigation of the impact of noise on standard fibre tracking algorithms

S. Schnell¹, B. W. Kreher¹, J. Hennig¹, and K. A. Il'yasov¹

¹Dept. of Diagnostic Radiology, Medical Physics, University Hospital Freiburg, Freiburg, Germany

INTRODUCTION: With the development of the Diffusion Tensor Imaging (DTI) technique algorithms for the reconstruction of neuronal fibre tracks evolved. Even with a limited signal to noise ratio (SNR) in DTI images, especially for single shot techniques, the fibre tracking algorithms are able to detect neuronal fibre bundles successfully and more research is done in order to dissolve complex structures such as fibre crossings. In this abstract the impact of noise on fibre tracking algorithms under varying SNR conditions is investigated. Evaluation was done on simulated data as well as measured data. Two fibre tracking algorithms were chosen, which are exemplary for the two most used tracking families in DTI world: the streamline and the probabilistic approaches.

METHODS: The measured DTI images were acquired on a 3 T Siemens MR Scanner. In order to abandon noise caused by living volunteers and to show reproducible results, a fibre-bundle phantom was used [1]. The phantom contained straight (Fig. 1) and spiral shaped fibre bundles, which were fixed in a container filled with water. A diffusion sensitive Spin-Echo EPI sequence with 31 (DE31) and 5 b0 images and 6 DE gradient directions averaged 5 times (DE6_5) was varied by changing the Inversion Recovery Time (TI). This results in DTI images with varying SNR while keeping the same conditions. The SNR value was determined in the b0 images and corrected with a factor of 1.53 for being Rician distributed. The effective b-value was 1000 s/mm². The in-plane resolution was 2x2 mm with a slice thickness of 2.5 mm. The measured results were to verify using results obtained from artificial data sets. For this, two different simulated 2D data sets were created. One data set contained a line representing straight fibre bundles and the other a circle (Fig. 2), representing curved fibre bundles. Both data sets were produced for DE31 gradient directions and varied by generated Gaussian white noise in order to achieve different SNR conditions. The image size was 100x100 pixels. Each SNR condition was repeated 100 times in order to show statistical relevant results.

After calculation of the diffusion tensors two different fibre tracking algorithms were tested: the streamline algorithm FACT (Fig. 2b) [2] and a probabilistic streamline-based algorithm (Fig. 1 and 2a) similar to PiCo [3]. For the FACT tracking a maximum angle of 53.1° was allowed. The applied probabilistic approach propagates through the tensor field after each iteration using the FACT algorithm. But instead of propagating along the main axis of the DT, the traversed direction was determined by random experiment. The underlying DT was sharpened by applying an exponent of 2 and was then used as density function for the random experiment.

The data processing was done using the DTI&Fiber Tools [4], where both tracking algorithms are implemented. The fibre tracking was started in a seed region. In order to quantify the results obtained by the different algorithms several end region of interests (ROI) at various distances were defined. For both algorithms a normalizing procedure was applied. The data were related to the probability or amount of fibres reaching the end ROI in the image with no noise (SNR = ∞). For both algorithms it was compared how success decreased with tracking distance or phantom shape.

RESULTS: The success of probabilistic and FACT tracking of the simulated data showed a decrease for decreasing SNR and longer distance. This was observed for the line phantom as well as the circle phantom. The same trend could be observed for the measured data (Figure 3). In addition, it could be observed that the success of tracking was influenced by the shape of the phantom (Table 1). The line phantom showed better results than the circle phantom. In the table below the SNR of the data sets is shown when tracking success was above 50, 75 and 90 % for the simulated line (Table 1a) and circle phantoms (Table 1b). The graph (Fig. 3) displays how the amount of fibres decreases for different distances depending on SNR in the simulated line phantom (DE31) and the measured straight phantom (DE6_5).

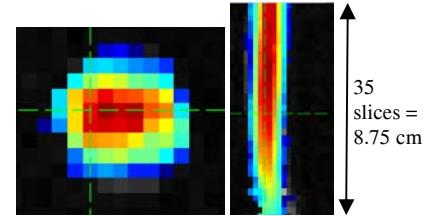


Figure 1: Example of an FA map of the measured straight fibre phantom with SNR = 41 and its probability map for DE6_5. The red colour means high and blue low probability values.

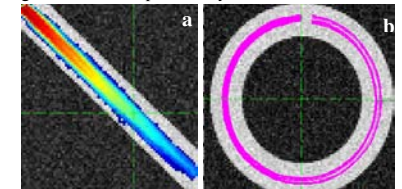


Figure 2: Both data sets shown here have an SNR of 18 and DE31. In 2a, FA map of the simulated line and the corresponding probability map are shown. In 2b, the FA map of the simulated circle is displayed together with fibres tracked by the FACT algorithm.

Tracking Alg	SNR _{50%}	SNR _{75%}	SNR _{90%}
distance l = 16			
FACT	7	13	34
Prob	8	14	22
distance l = 33			
FACT	12	24	64
Prob	14	23	43
distance l = 69			
FACT	18	36	96
Prob	21	32	64

Tracking Alg	SNR _{50%}	SNR _{75%}	SNR _{90%}
distance l = 29			
FACT	12	24	65
Prob	26	22	56
distance l = 59			
FACT	17	34	89
Prob	19	32	71
distance l = 110			
FACT	24	55	130
Prob	24	35	56

Table 1: The data sets being above 50, 75 and 90% of trackable fibres for FACT and probabilistic algorithm for several distances l depending on SNR. The SNR values are linear interpolated. Here only the results for the simulated phantoms are shown. Whereas table 1a. shows the simulated line and 1b the simulated circle.

DISCUSSION & OUTLOOK: The introduced investigation showed that, when reconstruction of neuronal fibres is goal of the DTI measurement and more than 75% of possible fibres are to be detected in rather straight fibre bundles, such as the spinal cord, this can only be achieved for DE31 when having SNR above 35 for a distance of 69 pixels (for slice thickness = 2mm this corresponds with 13.8cm). For curved fibre bundles such as the Corpus Callosum it is recommended to measure DTI images above SNR = 33 for a distance of 59 pixel. Both tracking algorithms, FACT and probabilistic behaved similar for all noise conditions and two different shapes in the simulated data sets. Except for longer distances and if more than 90% of possible tracks are wanted to be detected, the probabilistic algorithm seems to be more stable. The measured results showed the same tendency. Due to time constraints and the possibility to easily repeat simulations, these were preferred and only one measurement per condition was performed. This was done in order to examine whether or not measured results confirm the simulated results. Though, the measurement and simulations are not directly comparable. Only 2-D simulations were done with no complicated structure in order to have the opportunity to repeat the simulations in high numbers. Therefore geometry of the simulated and measured phantoms is not similar and not comparable. However, the performance under various noise conditions of the tracking algorithms compared within the simulated data is surprisingly similar and it could not be found that one or the other algorithm is superior. The applied tracking algorithms were used exemplary, but there exist several similar and extended models. In this paper it was only shown how these specific algorithms behave, which gives a tendency for the two tracking families. Nevertheless, one should investigate these other models in order to confirm this statement. In addition, further investigations of the behaviour of tracking algorithms at different noise levels in complex fibre crossings as well as extended noise models, such as physiological noise or image distortion should be done.

REFERENCE

[1] Lorenz R., et al. Proc. ISMRM. 14, # 2738, (2006)
 [2] Mori S, et al.; Ann Neurol, 45:265 (1999)

[3] Parker G.J.M., et al, JMRI 18:242-254 (2003)
 [4] Kreher W., et al. Proc. ISMRM. 14, # 2758, (2006)

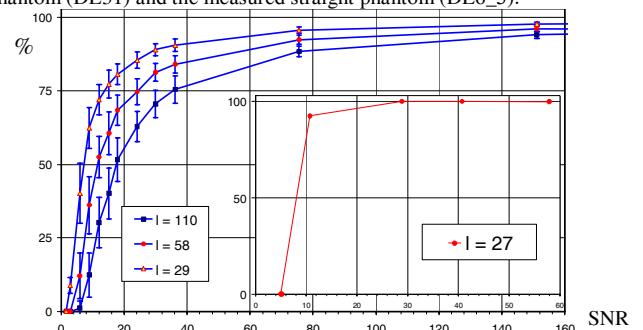


Figure 3: Comparison of the mean amount of fibres in percentage reaching end ROI positioned at different distances l. Here, the phantoms were tracked using the FACT algorithm. The blue line represents the simulation (DE31) and the red the measured result (DE6_5).